Soft Matter

Accepted Manuscript

ROYAL SOCIETY OF CHEMISTRY

www.rsc.org/softmatter

Soft Matter

ARTICLE

Multi-region to single region shear thinning transitions in drying PEDOT:PSS dispersions: Contributions from charge density fluctuations

Received 00th January 20xx,
Accepted 00th January 20xx

DOI: 10.1039/x0xx00000x

www.rsc.org/

Piramuthu Raja Ashok. R, Mathew Shaji Thomas and Susy Varughese†

The multiple shear thinning behaviour observed in the dispersions of the conducting polymer, poly(3,4-ethylenedioxythiophene)-poly(styrenesulfonate) (PEDOT:PSS) in water during the drying process is explored. PEDOT:PSS dispersions in water can be non-stoichiometric polyelectrolyte complexes (PEC) with free polyanion (PSS) chains resulting in scrambled egg conformations. They also behave as charged colloidal particles. The behaviour of PEDOT:PSS dispersions as PEC and charged colloidal systems during the drying is analyzed using rheology and TEM, zeta potential, conductivity, pH, dynamic light scattering (DLS) and rheo-small angle light scattering (rheo-SALS) information. Rheological behaviour is found to have significant contributions from conformational changes in the PEDOT:PSS PEC due to charge density fluctuations affecting the electrostatic persistence length, l_e. A low concentration regime with multiple shear thinning behaviour and a high concentration regime with single shear thinning behaviour were observed. The PEC behavior of PEDOT:PSS is further explored by charge neutralizing the dispersions with salts

Introduction

Poly(3,4-ethylenedioxythiophene):poly(styrene sulfonate) (PEDOT:PSS) is a widely accepted charge transport material in organic light emitting diodes (OLED), organic solar cells, memory storage devices, field effect transistors and other applications in plastic electronics.[1] The performance of multi-layer OLEDs and other opto-electronic devices can be significantly affected by small changes in the charge injection efficiency which originates from the microstructural changes in the constituting layers. Although there are many studies on the optoelectronic properties of PEDOT:PSS,[2-4] the evolution of its electronic properties and morphology during processing,[5-7] and the optimal processing parameters[7,8] for specific device architectures are yet to be understood in detail. PEDOT:PSS dispersions in water are processed using techniques such as spin coating,[7] gravure printing,[9] inkjet printing,[8] solvent casting,[10]etc. In all these processes, dispersions are dried to arrive at the final device feature. The ink dispersions show different types of rheological behaviour during various stages of their preparation, storage, printing and drying. The low shear rate regions represent stability of material; sedimentation processes, phase separation and structure retention during storage conditions. The high shear rate regions represent stages such as jetting and subsequent drop ejection through inkjet nozzle during the printing process.

The microstructure of PEDOT:PSS dispersion, a polyelectrolyte complex (PEC) in water, comprises of cationic, PEDOT molecules electrostatically bound to the PSS polyanions along with excess PSS chains, enabling stable dispersions at low polymer concentrations (<5wt. % solids).[4,11] Due to the electrostatic interactions between the PEDOT and the PSS chains a core-shell structure with PEDOT core and PSS shell forms micro-gel particles (10 nm-1μm)[1] in water with minimum interactions between PEDOT and water (Scheme 1). The non-stoichiometric ratio of PSS to PEDOT also results in scrambled egg conformation of the PEDOT:PSS in water[1] which remains as colloidal particles at dilute concentrations (<0.1 mg/mL).[12] Therefore, in addition to being a non-stoichiometric PEC in water, PEDOT:PSS dispersions can also be considered as charged colloidal dispersions along with free PSS polyanions.[13]

[a] *Polymer Engineering and Colloids Science Laboratory, Department of Chemical Engineering, Indian Institute of Technology Madras, Chennai- 600036, India. Email: susy@iitm.ac.in*
†. Corresponding Author

Electronic Supplementary Information (ESI) available: Shear hysteresis of dilute PEDOT:PSS dispersions. Torque measurements during the steady shear rheological measurements and the particle size data from dynamic light scattering (DLS) measurements before and after shearing process in a Vortex mixer. Table showing the variation of electrostatic persistence length, *le* of PEDOT:PSS dispersions with the addition of NaCl and $CuCl_2$. The optical micrographs of $CuCl_2$ added PEDOT:PSS dispersions are included. See DOI: 10.1039/b000000x/

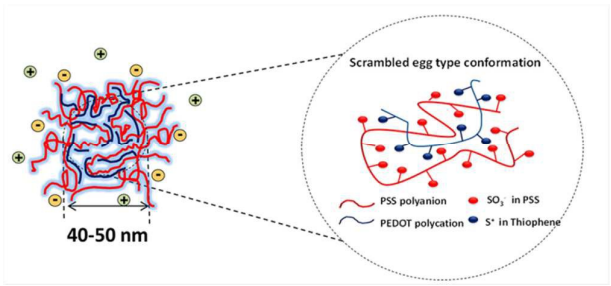

Scheme 1 Schematic representation of PEDOT:PSS gel particle with counter-ions. The non-stoichiometric PEC showing the scrambled egg type conformation.

In steady shear rheology, dispersions of soft deformable colloidal spheres exhibit mild Newtonian plateau followed by shear thinning.[14] However, polyelectrolytes are usually characterized by an extended Newtonian plateau followed by shear thinning behaviour. For the colloidal dispersions, the particle-particle interactions govern the shear response at any given volume fraction. The shear thinning behaviour is due to the breaking up of particles or clusters (at high volume fractions) into smaller clusters/individual particles.[14,15] The interactions in PEDOT:PSS dispersion are known to have short range attractions between PEDOT:PSS gel particles and long range repulsions among the free PSS anions and the gel particles. Previous studies have shown that dilute PEDOT:PSS (<1.3 wt%) dispersions exhibit shear thinning behaviour at high shear rates.[16-18]

The conformation of PEDOT molecule is very important for the device performance, for example, more linear or extended the conformation of the PEDOT chain is, the higher the electronic conductivity could be in a device.[19] The PSS anions adopt two types of conformations in the dilute PEC (<5wt%): a coiled conformation in the shell and a linear/extended chain conformation for the free PSS anions due to Columbic repulsions.[20-21] In dilute dispersions, the gel particles are stabilized against further coagulation via electrostatic repulsion from excess PSS in the shell. It is also possible to have H-bonding between -HSO_3 groups of adjacent PSS-rich shells.[11] In this context, the conformational changes during the course of drying of PEDOT:PSS (processing) will be interesting due to the different charge compensation processes and the charge density fluctuations. To elucidate the conformational changes during the drying of the PEDOT:PSS dispersion, we investigate the contributions of charge compensation processes through rheology, supported by experimental data from dynamic light scattering, microstructure from STEM, zeta potential, ionic conductivity and pH measurements. In the present work, dilute PEDOT:PSS dispersions in water were allowed to dry in air at 60 °C. During the drying, the concentration of the polymer changes and the conformations of the constituent PEC (PEDOT:PSS) as well as the free PSS anions are expected to change. Rheological studies (under steady and dynamic shear) of these dispersions carried out after drying for specific intervals of time show interesting characteristics which have not been reported for a PEC drying process. Contributions of charge density fluctuations to he observed multi region shear thinning behaviour and different relaxation time regimes are investigated through charge neutralization using salt.

Materials and Methods

PEDOT:PSS (1.3 wt. % solids; M_w= 2,80,000 as provided by the supplier) dispersion in water was purchased from Sigma Aldrich Ltd, USA (Lot #MKBP6289V). The ratio of PEDOT to PSS is 0.5 to 0.8 wt. %. The free PSS in the dispersion is 100% H-type. The polymer dispersion was stirred at room temperature (32 °C),sonicated for 2h and then filtered through a 5 µm Whatman® filter paper to remove the aggregated particles, prior to drying and rheological experiments. The concentration of polymer after the filtration process was found to be 1 wt. % and is dependent on the time of sonication process. Solutions of sodium chloride (NaCl) and copper chloride ($CuCl_2$) (Merck, India), were prepared in different ionic strengths (0.2 mM to 0.7 M) using MilliQ® water and were added to PEDOT:PSS dispersion to investigate the charge neutralization process and the changes in persistence length. After the addition of salt, the dispersion was mixed in a vortex mixer and sonicated for 5 min prior to experiments. A known weight of the polymer dispersion (4g) was taken in a glass petridish (dia - 45mm, depth – 12 mm) and dried in a hot-air oven at a temperature of 60±1 °C and 68% RH. Rheological studies were carried out on the drying dispersions under dynamic and steady shear conditions using a stress controlled rheometer (Anton Paar Physica MCR 301). A cone and plate geometry with 25 mm diameter, 1° cone angle and 0.052 mm initial gap was used. The viscosity of the dispersions was measured at shear rates ranging from 0.001 to 1000 s^{-1} at 25 °C. Strain amplitude sweep tests from 0.1% to 100% were carried out at 10 rad s^{-1}. Solvent traps were used to avoid evaporation of water during the rheological measurement. Small Angle Light Scattering (SALS) attachment (Anton Paar) was used along with the rheometer to follow the structural changes during shearing. The rheo-SALS setup consists of a laser of wavelength 658 nm, a transparent glass measuring cell and parallel plate (dia -43 mm) geometry, the focusing optic for the scattered light and the detection unit including the CCD camera. The particle size, zeta potential and the conductivity measurements of the dispersions were carried out using Horiba SZ-100 particle analyzer (dynamic light scattering (DLS)). The pH of the dispersions was measured using a pH tester (pH Checker, HANNA instrument) within accuracy of 0.05 pH. The pH measurements were performed for three separate drying experiments to ensure reproducibility. To study the rheology during drying, dispersions dried for different time intervals in a petridish were drawn using a spatula at different time intervals after stirring and allowed to rest for 30 s. Beyond a certain duration of drying, the pH, particle size and zeta potential measurements could not be carried out due to high viscosity build-up in the dispersion.

To probe the microstructure at low and high concentrations, TEM characterization was carried out at 200 kV using FEI Tecnai20 G2 (FEI, Netherlands) transmission electron microscope. The polymer dispersion was diluted 10-fold with

DI water and one drop of clear water-like dispersion was dispensed on the copper grid and allowed to dry for an hour. For high concentrations, sample dried for 60 min was taken from the oven and a drop was dispensed on the copper grid and left for drying.

The volume fraction (ϕ) of the polymer during drying was estimated using gravimetric method. The weight of the samples were recorded as the drying progressed using a Sartorius CPA225D analytical balance sensitive to 0.01 mg. Since PEDOT:PSS are swollen micro-gel particles in dispersion, the volume fraction thus obtained may not be accurate measure of the particle concentration. The particle size keeps changing depending on the drying state and therefore instead of the volume fraction, ϕ an effective gel volume fraction, ϕ_{eff} is used which is defined for soft deformable particles: $\phi_{eff} = nV$, where n is the number density of the particles, and V is the volume of the un-deformed particle in the dilute suspension.The polymer mass concentration, c (g/L) from the gravimetric data is converted into ϕ_{eff} using the specific viscosity η_{sp} obtained when $c \rightarrow 0$,[20]

$$\eta_{sp} = \frac{\eta_0 - \eta_s}{\eta_s} = \beta_1 c = \alpha_1 \phi_{eff}. \quad (1)$$

Where η_0 and η_s are the zero shear viscosities for the dispersion and the medium respectively, α_1 and β_1 are coefficients. A straight line fit to the Einstein's relation would give us the coefficient, k ($k = \beta_1/\alpha_1$) relating ϕ_{eff} and c. The measured ϕ_{eff} is fitted using the Batchelor's expression, $\eta_{rel} = \frac{\eta_0}{\eta_s} = 1 + 2.5\phi_{eff} + 5.9\phi_{eff}^2$. For the estimation of the effective volume fraction, the dispersions are considered locally electro neutral everywhere in the dilute limits. For this purpose, dilute concentrations of PEDOT:PSS were prepared by adding de-ionised water and the specific viscosity of the dispersion was determined from steady shear experiments using the rheometer. The variation of effective volume fraction estimated thus and the solids concentration of PEDOT:PSS obtained from gravimetric measurements during the drying at 60 °C are shown in Fig. 1. The volume fraction referred to hereafter corresponds to the effective volume fraction (ϕ_{eff}).

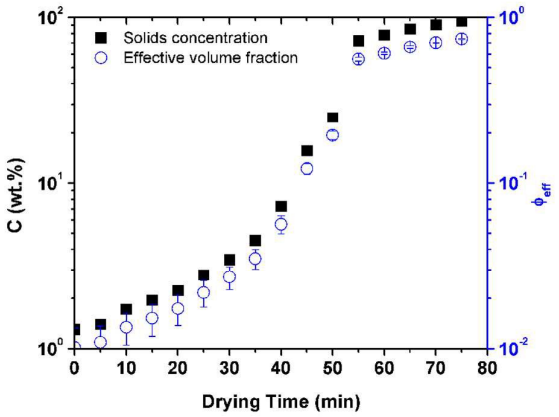

Fig. 1 Variation of solid concentration and effective volume fraction ϕ_{eff} of PEDOT:PSS dispersion with time during drying in air at 60 °C.

Results and Discussion

Rheological studies were carried out on PEDOT:PSS dispersions dried for various time intervals. Drying process can be considered equivalent to changing the concentration of the polymer and hence a change in effective volume fraction (ϕ_{eff}) is used in the discussion. Zeta potential, H+ concentration and conductivity data are used for monitoring the conformation changes and charge density fluctuations in PEDOT:PSS PEC system as the drying process progresses. Steady shear rheology of dilute dispersions as well as of dispersions in the presence of monovalent and divalent salts (NaCl and $CuCl_2$) was studied to understand the charge compensation processes in the PEC and its contribution to the rheological behavior. Rheo-SALS data is used only for the qualitative comparison of the observed changes during shearing.

Multi-region shear thinning behavior

The steady shear rheology studies show different behavior at different ϕ_{eff}. Dilute PEDOT:PSS dispersion (at 1.0 wt.%; ϕ_{eff}= 0.01) exhibits multiple shear thinning regimes (N1, N2 (with three sub-regions, R-I, R-II, R-III) N3 and no Newtonian plateau) with the transition at different critical shear rates (Fig. 2). The entire shear thinning regimes (N1, N2 and N3) as well as the sub-regions could be modeled using the Power law model with different n values indicating interactions of varying nature contributing to the shear thinning (Table 1). In the N1 regime, the apparent viscosity of PEDOT:PSS dispersion decreases from 0.5 Pa.s to 0.1 Pa.s with n = 0.5. Regime N2 can be considered to have three sub-regions (R-I, R-II and R-III) with different Power law indices and the viscosity decreases by an order of magnitude when the shear rate is increased above 1 s^{-1} showing more pronounced shear thinning. For shear rates above 20 s^{-1} (regime N3), the viscosity of the dispersion was found to vary within one order of magnitude with n = 0.87. All the three regions and sub-regions were further probed with shear and recovery experiments. Shearing of PEDOT:PSS dispersions is known to break down the PEDOT:PSS gel particles resulting in particle size reduction.[1] The average size

of PEDOT:PSS gel particles was reported to decrease from 380 nm to 23 nm at the end of a shearing process. The notable hysteresis (in Fig. S1) observed near R-II to R-III indicates aggregate break-down at these shear rates. No hysteresis was observed for other shear rate regimes. No studies are reported correlating the viscosity changes associated with such processes and the contributions of charge-mediated assembly and breakdown in PEDOT:PSS dispersions. In the present study, an independent shearing experiment carried out on PEDOT:PSS dispersion at 1000 s^{-1} in a vortex mixer for 15 min showed a gel particle size reduction from 550±2.5 nm to 50±3 nm (Fig. S2). Therefore, the shear thinning behavior in regime N2, is attributed to the breakdown of the aggregated gel particles. The dilute dispersion rheology shows that the regime N1 corresponds to Newtonian or at rest (low shear) behavior, N2 to the breakdown of aggregates of colloidal gel particles (shear rate ~0.1 to 20 s^{-1}) and N3 to the alignment of gel particles in the shear direction (shear rates > 20 s^{-1}). Rheo-SALS images at different critical shear rates (Fig. 2) show the microstructural changes during the shear thinning. The change of the 2-D pattern from circular to elliptical indicates a more oriented structure as the shear rate is increased.

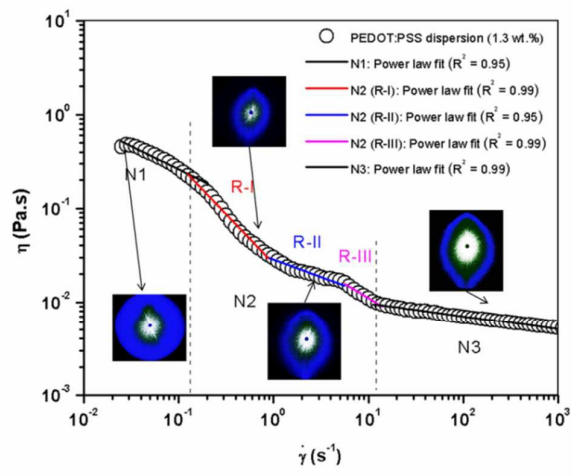

Fig. 2 Shear rate dependence of apparent viscosity of PEDOT:PSS dispersion (ϕ_{eff} = 0.01) in water. The dotted line indicates the transition through N1, N2, N3. The solid lines are the power law fit in each of the shear thinning regimes.2-D SALS pattern obtained at different shear rates show circular to elliptical change in the pattern. The estimated zero shear viscosities are approximate since the PEDOT:PSS dispersions are highly sensitive to the shear thinning effect in the low shear region. To ensure the accuracy of measurements in the low shear rate range, the torque values were monitored during the experiments and were found to be within the machine limits (Fig. S3).

Table1. Power law parameters and critical shear rates determined from the steady shear viscosity measurements for PEDOT:PSS dispersion during the initial drying process

Drying time (min)	ϕ_{eff}	Power law index in the shear thinning regime				
		N1	N2			N3
0	0.01	0.5	0.06	0.63	0.4	0.87
15	0.015	0.73	0.19	0.82		0.75
20	0.017	0.98	0.46	0.32		0.86
25	0.021	0.81	0.34			0.80
30	0.027	0.39	0.61			0.8
35	0.035	0.94	0.23	0.49		0.78
40	0.056	0.96	0.1	0.11		0.42

Multi-region shear thinning behavior is observed in associative polymer systems such as polyacrylamides[21] and hydrophobically modified alginates.[22] Distinct multiple shear thinning regimes associated with structural changes are also exhibited by liquid crystalline polymers due to phase transformations during shearing.[23] The multi-region shear thinning behavior observed in PEDOT:PSS dispersions during the drying process is found to be very distinct from that of the typical rheological behavior of liquid crystalline systems and associative polymer systems.

Rheology during drying

Once the water starts evaporating from the PEDOT:PSS system, the three sub-regions found in the N2 region of dilute dispersion changes to two sub-regions (R-I, R-II) for ϕ_{eff}=0.015 and then switches to one sub-region (R-I) at ϕ_{eff} = 0 021 (Fig. 3 (a) and (b)). Again at ϕ_{eff} = 0.035, it changes to two sub-regions in the N2 region. Three different shear rate dependent behavior regimes are observed during the entire drying period of 75 min (Fig. 3 and Fig. 4): (i) multi-region shear thinning without Newtonian plateau in the case of dilute dispersions (ii) A Newtonian plateau followed by multi-region shear thinning behavior for drying periods, 20 to 40 min (ϕ_{eff} = 0.017 to 0.056, regions:N1, N2 with sub-regions and N3) and (iii) A short Newtonian plateau followed by a single-region shear thinning for drying periods more than 45 min (ϕ_{eff}> 0.12, regions: N1 and N2). The shear thinning behaviour during the later stages of drying (> 45 min; 0.12 <ϕ_{eff}< 0.74) could be explained using Carreau model: $\eta = \frac{\eta_0 - \eta_\infty}{[1+(\lambda\dot{\gamma})^2]^n} + \eta_\infty$, where η_0, η_∞, λ and n are the zero shear viscosity, infinite shear viscosity, characteristic relaxation time and power law index respectively. The characteristic relaxation time λ increases with drying time (Table 2).

A short Newtonian plateau (N1) appears at low shear rates for drying times >5 min (Fig. 3(a)-(d) with an increase in low-shear viscosity values. While increasing the drying time from 35 to 40 min, there is a dramatic two-orders of magnitude increase in the zero-shear viscosity values(0.43 Pas to 125 Pas) as well as a reduction in the critical shear rate from 0.45 s-1 to 0.02 s^{-1} (N1 to N2 region) and from 15.8 $s^{-1}$to 9.2 s^{-1} (N2 (R-II) to N3 region). The building up of the viscosity by two orders of magnitude during a very short interval of drying time (from 30 to 35 min) indicates the interplay of changes in conformation and aggregation behavior rather than colloidal aggregation alone.[21] At shear rate,15.8 s^{-1} where the transition from N2 to N3

occurs, the intensity of the scattering pattern increases. The fluctuations in *n* can be conjectured based on the amount of water present during 20 to 40 min of drying. As the dispersion was dried further (45 to 75 min, ϕ_{eff} = 0.056 to 0.74) the zero shear viscosity increased from 0.45 Pa.s to 8610 Pa.s and the power law index *n*, increased from 0.35 to 0.5 respectively indicating weaker shear thinning response. Rheo-SALS patterns obtained at different shear rates for ϕ_{eff} = 0.66 is shown in Fig. 4 (b). At low shear rates, 2-D scattering patterns look similar and as the shear rate is increased, the elliptical pattern starts to appear and the area of the ellipse decreases with further increase in shear rates indicating alignment of structures in the direction of shear.

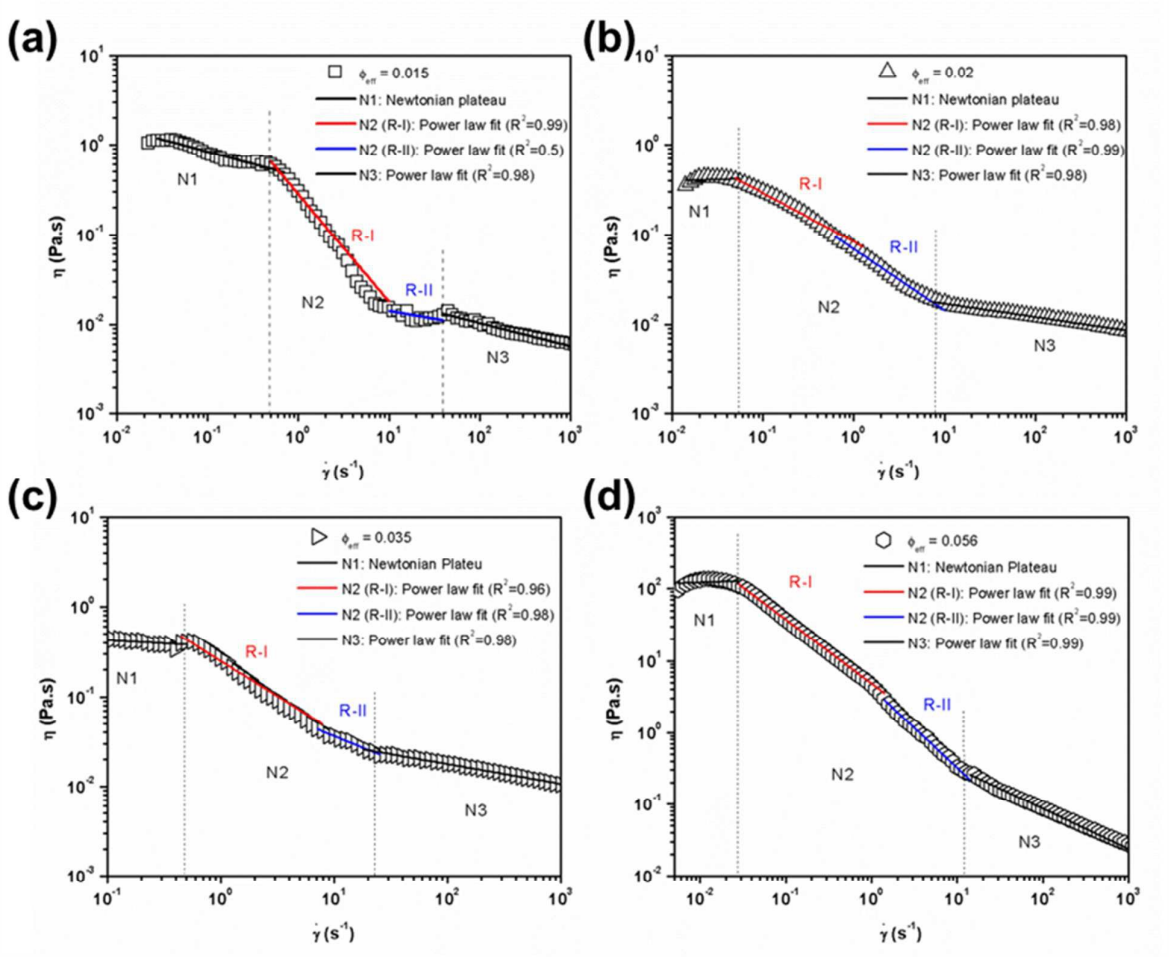

Fig. 3 Shear rate dependence of apparent viscosity of PEDOT:PSS dispersion in water at (a) ϕ_{eff} = 0.015, (b) ϕ_{eff} = 0.02, (c) ϕ_{eff} = 0.035 and (d) ϕ_{eff} = 0.056. The dotted line indicates the transition from one thinning regime to another (N1, N2 and N3). The black, red, blue and magenta lines indicate the power law fit for different regimes N1 and N3, N2(R-I), N2(R-II) and N2(R-III) respectively

.

Soft Matter

ARTICLE

Table 2. Parameters for Carreau Model (PEDOT:PSS dried for > 45 min)

Drying Time (min)	ϕ_{eff}	Power Index, *n*	Zero Shear Viscosity, η_0,(Pa.s)	Critical shear rate, $1/\lambda$ (s^{-1})
45	0.12	0.35	45.4	0.045
50	0.19	0.38	102	0.044
55	0.56	0.41	959.5	0.02
60	0.60	0.43	3158	0.015
65	0.66	0.49	3750	0.027
70	0.70	0.48	6032	0.025
75	0.74	0.5	8590	0.018

After 60 min of drying, shear thinning was more pronounced with increasing volume fraction (ϕ_{eff}> 0.56) indicating that the assembly of PEDOT:PSS gel particles formed are weakly connected. Polyelectrolytes show extended low shear Newtonian plateau and the critical shear rate for shear thinning decreases with increasing concentration.[22] In the case of PEDOT:PSS, the low shear Newtonian plateau is not prominent for different concentrations and the critical shear rate for shear thinning does not change significantly with increasing concentration (Table 2). Colloidal systems at high concentrations (hard spheres, soft micro-gel particles and particles with electrostatic interactions) exhibit yield stress behavior at low shear rates due to the maximum packing factor of the particles in a given volume.[14, 21, 23] However, even during the final stages of drying of PEDOT:PSS dispersions (high concentrations, ϕ_{eff}= 0.74) did not show any yield stress behavior although closely packed aggregates and networks might have formed. The rheological behavior of PEDOT:PSS dispersions points to independent contributions from PEDOT:PSS as a non-stoichiometric PEC and as a charged colloidal dispersion of micro-gel particles. Further analysis takes into account the conformation/structural changes with charge density variation as the water content in the system changes.

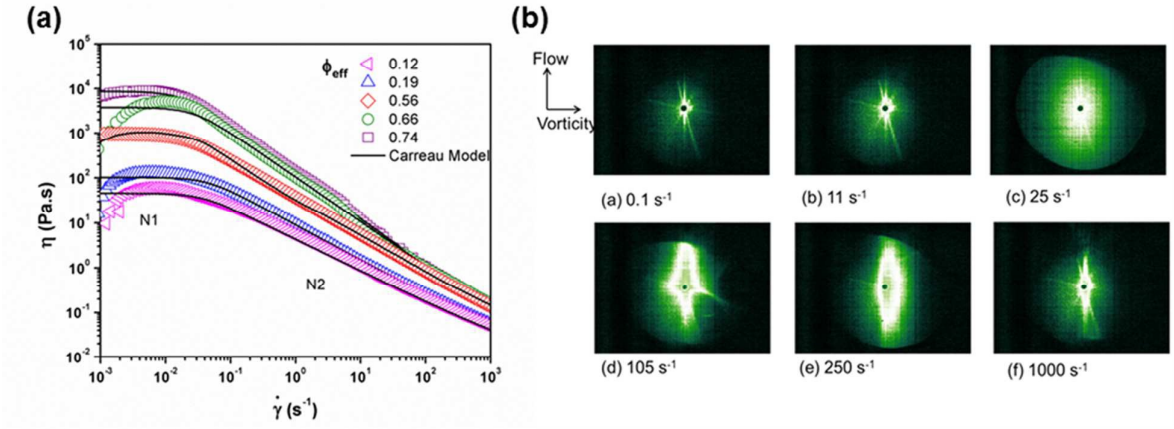

Fig. 4 (a) Apparent viscosity for PEDOT:PSS dispersion during the later stages of drying (45-75 min). The response is modeled using Carreau model. (b) 2-D SALS pattern of PEDOT:PSS dispersion at ϕ_{eff}= 0.66 at different shear rates.

When the dispersion is sheared, there are multiple interaction mechanisms responsible for the stability of the dispersion – electrostatic interactions inside the gel particle, H-bonding among the gel particles, association/dissociation of protons from/to free PSS anions and water.

Electrostatic interactions during drying

To understand the contribution of various charges on the observed steady shear rheological behavior due to evaporation of water from the dispersion, pH, zeta potential and conductivity data were obtained for different ϕ_{eff}. At ϕ_{eff} = 0.01 the zeta potential of PEDOT:PSS dispersion is -82.5 mV suggesting the net negative charge due to the non-stoichiometry of PEDOT and PSS in the complex. From Fig. 5(a), it is evident that as the water evaporates from the dispersion, there are fluctuations observed in the zeta potential (+78.5 mV for ϕ_{eff} = 0.015 to -19.8 mV for ϕ_{eff} = 0.027) and change in the ionic conductivity of the dispersion (8.4 mS/cm for ϕ_{eff} = 0.015 to 5.5mS/cm for ϕ_{eff} = 0.027) until the drying process is complete.

The variations in the counter-ion concentration (Fig. 5(b)) was observed to change from 0.007 M (ϕ_{eff} = 0.01) to 0.023 M (ϕ_{eff} = 0.015) corroborating well with the fluctuations in zeta potential values. At 25 min of drying (ϕ_{eff} = 0.021), large

number of counter-ions (peak in Fig. 5(b)) were released into the medium and thereafter with increasing drying time, the number of counter-ions kept decreasing until it reached a constant value. The concentration of the counter ions in the dispersion was determined from the measured pH values. These fluctuations are clear indications of the changes in the charge density of PEDOT:PSS due to the release or capture of counter-ions (H+) in the dispersion during the drying process. The zeta potential approached zero between 0.027 $<\phi_{eff}<$ 0.056 suggesting that the dispersion reached charge neutralization point. As the charge neutrality point is approached (ϕ_{eff} = 0.056), the low shear viscosity values also become very high (Fig. 5(b)) suggesting the formation of secondary aggregates from fragmented, non-connected PEC particles (ϕ_{eff} = 0.035). Due to the continuously changing solvent environment (due to the evaporation of H_2O), it is difficult to identify the exact charge neutralization point during the drying process. Due to the evaporation of water, the polymer chains come closer and the electrostatic repulsion among PSS anions also increases. The net negative charge of the complex continuously changes during the drying process due to the strong electrostatic field generated by the PSS anions in the changing water environment resulting in minimization of the interaction between the PEDOT and the PSS molecules. This favors the switching of positive and negative potentials in the complex. However, the free PSS chains and the loops and ends of the PSS present in the PEC particle are not the only contributors to the interesting rheology of the PEDOT:PSS dispersion.

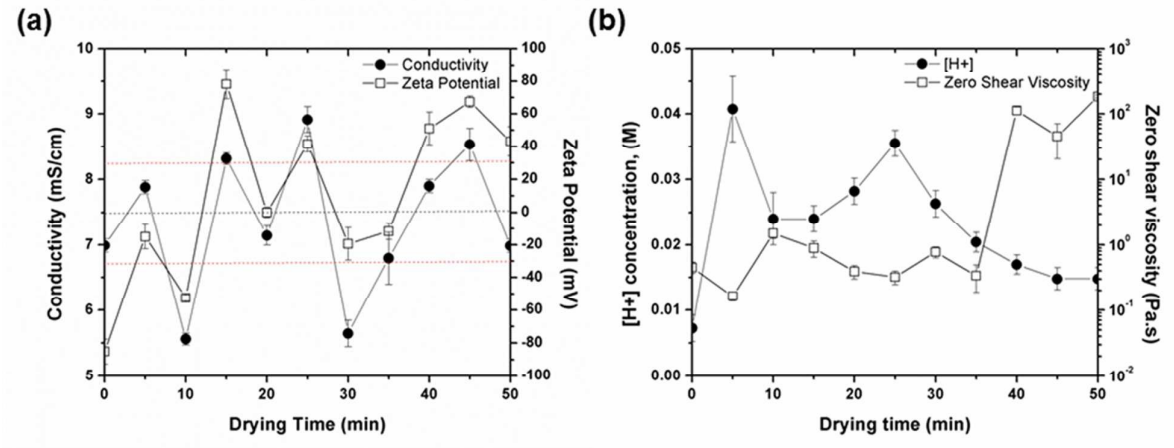

Fig. 5 (a) Conductivity and zeta potential of PEDOT:PSS dispersion during the initial stages of drying process. The line is to guide the eye. **(b)** Zero shear viscosity and proton concentration for PEDOT:PSS dispersion during the initial stages of drying.

Effect of charge neutralization

To investigate the contributions of charge density on the rheological behavior of PEDOT:PSS dispersion during drying, a monovalent and a divalent salts were added. At low concentrations, both the salts did not affect the viscosities significantly (Fig. S4). However, the divalent salt ($CuCl_2$) was found to have more prominent effect on the low shear viscosity (upto two orders of magnitude) at 0.05 M for $CuCl_2$ in comparison to the monovalent salt (NaCl) at 0.4 M. Divalent cations were found to be more effective than the monovalent counterparts in screening the electrostatic charges in PEDOT:PSSdispersions.[24] Further, the divalent salt added dispersion showed multi-region shear thinning at low salt concentrations (< 0.05M) and single region shear thinning at high salt concentrations (> 0.05M) while the monovalent salt added dispersion showed two-region shear thinning at all the concentrations. The power law indices (Table 3) for low concentrations of divalent salt added dispersions (< 0.003M) suggest that the nature of shear thinning in each of the regimes are similar to that of the salt-free dispersion. And for

0.003M $CuCl_2$ added dispersion (Fig. 6), N2 regime comprised of three sub-regions (R-I, R-II and R-III) similar to that of the salt-free dilute dispersion.

Table 3. Power law indices of PEDOT:PSS with different concentrations of added NaCl and $CuCl_2$

Salt concentration (M)	Power Law index (*n*)						
	N1	N2: R1	N2: R2	N2: R3			N3
Salt-free	0.5	0.06	0.63	0.4			0.87
	NaCl		$CuCl_2$				
	N1	*N2*	*N1*	*N2*			*N3*
0.0002	0.65	0.89	0.61	0.37			0.87
0.0006	0.67	0.86	0.78	0.94			0.88
0.003	0.74	0.86	0.6	0.2	0.5	0.01	0.83
0.007	0.60	0.89	0.73	0.07			0.6
0.05	0.52	0.66	0.76	0.13			-
0.1	0.56	0.59	0.93	0.01			-
0.4	0.26	0.51	0.47	0.05			-
0.7	0.31	0.48	0.9	0.5			-

The added salt ions interact with the anionic charges of the PSS polyelectrolyte inducing changes in conformation (due to screening of anionic charges) of the polymer in dispersion which result in a change in the viscosity. Eventually, a salt concentration is reached where the number of added salt ions equals (charge neutralization), then exceeds, the number of free counter-ions in the dispersion (high salt limit). Once the high salt limit is attained, the addition of more salt has no effect on the polymer conformation and, thus, little effect on the rheology. Here, the high salt limits are 0.4M for NaCl and 0.05M for $CuCl_2$. At 0.05M $CuCl_2$, the dispersion shows the maximum zero shear viscosity (Fig. 7) and with further addition of salt the viscosity is lower at all the shear rates. In addition, at low shear and at high shear rates more prominent Newtonian plateaus appear with the infinite shear viscosity approaching that of water. Optical micrographs of the dispersions with the salt showed large sized aggregates (~50 µm) with more transparent surrounding medium (Fig. S5).

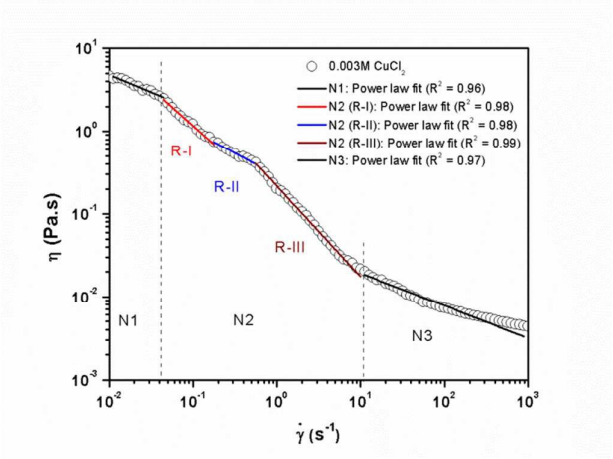

Fig. 6 Shear rate dependence of apparent viscosity of PEDOT:PSS dispersion in water with the addition of 0.003M $CuCl_2$. The dotted line indicates the transition from one thinning regime to another (N1, N2 and N3).

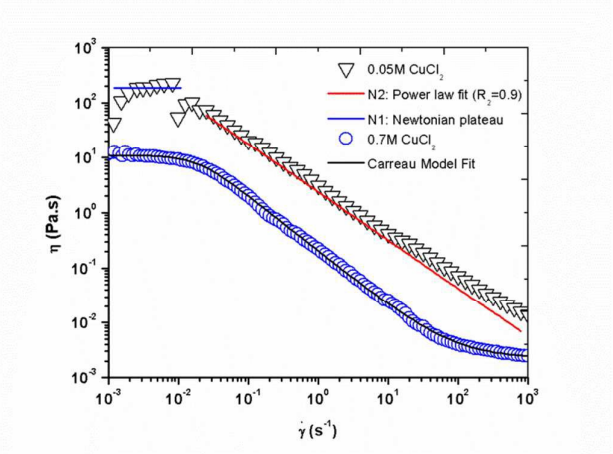

Fig. 7 Shear rate dependence of apparent viscosity of PEDOT:PSS dispersion in water with addition of $CuCl_2$ 0.05M and 0.7M

Salt addition vs drying process

Fig. 8 shows the comparison of the shear rate dependence of viscosity of PEDOT:PSS dispersion for salt added and drying (40 min) cases. At 0.05M concentration of $CuCl_2$, the shear rheology profile compares well with that of dispersions dried for 40 min. From the zeta potential measurements during the drying process, a notable shift from negative to positive surpassing zero potential was observed for 35 to 45 min of drying with corresponding increase in the viscosity of the dispersion. These observations indicate that the microstructure of the dispersion dried for 40 min is comparable with that of the 0.05M $CuCl_2$ added dispersions. Fig. 9 compares the particle sizes obtained from DLS technique for the dispersion with salt and dispersions without salt during the drying process. Similarities in the particle size evolution of the drying dispersion and the salt-added dispersion further confirms the effect of charge density fluctuations on the microstructure of PEDOT:PSS. The inset in Fig. 9 shows the particle size for different dilutions of the dispersion and the average particle size is about 30-50 nm. In the presence of salt, the screening of charges leads to associative phase separation in PEC gel particles. However, in the absence of salt (such as the drying process) the charge compensation processes are entropy-driven due to the strong mismatch in the charge densities and the full binding of PEDOT and PSS chains rather than a strictly local binding.[25] This leads to similar steady shear response in the case of charge neutralized PEDOT:PSS and the dried one. This indicates the role of electrostatic charges in the observed fluctuations in steady shear viscosity during the drying process.

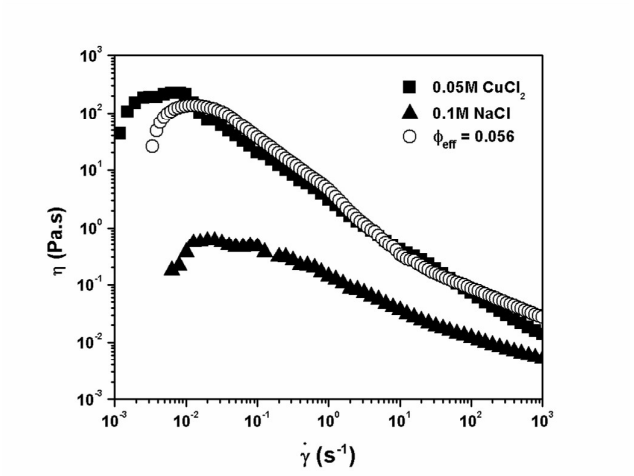

Fig. 8 Shear rate dependence of apparent viscosity for PEDOT:PSS dispersion under charge neutralization conditions. Open symbols for dispersion dried for 40 min (ϕ_{eff} = 0.056) and closed symbols for dispersions with 0.05M $CuCl_2$and 0.1M NaCl.

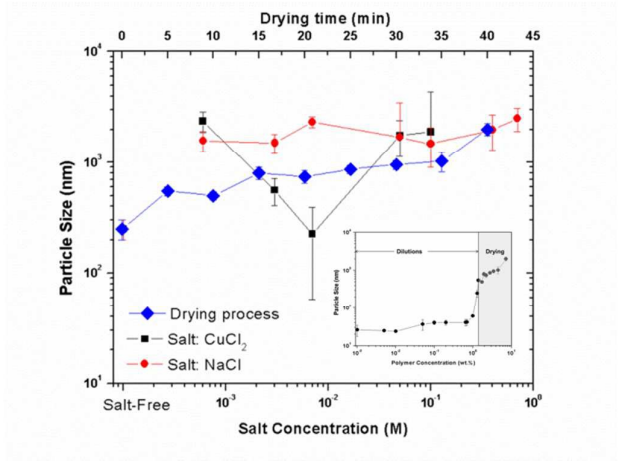

Fig. 9 Particle size data from DLS characterization of PEDOT:PSS dispersion during drying process and dispersion with added monovalent and divalent salts. The inset shows the change in particle size data for PEDOT:PSS dispersion as a function of concentration at different dilutions progressing towards complete drying.

Conformation changes in PEC

The charged colloid perspective does not explain the observed multi-region shear thinning for concentrations < 0.056. Therefore, an analysis based on the PEC structure of PEDOT:PSS is followed. The contribution of H+ ions to the conformations of the PEC and a polyelectrolyte in water are different. Dimitriev et al demonstrated that in very dilute dispersions of PEDOT:PSS (10^{-3} wt.%), it takes an extended conformation which changes to a coiled conformation at 10^{-1} wt.%.[26] At these corresponding concentrations, the pure PSS anions which are present along with PEDOT will also change from an extended to less-coiled conformation. At 1 wt.% (ϕ_{eff} =0.01), the PEDOT:PSS takes a scrambled egg type conformation with the free PSS chains adopting a stretched conformation.[1] As the water content decreases due to drying, more PSS anions become protonated (Fig. 5(b)) and take more coiled conformation. The conformations of a polyelectrolyte can vary with the electrostatic persistence length (l_e) and the Debye screening length (κ^{-1}).[27] Using electrostatic blob length, ξ= 0.55 nm, we get $\kappa\xi = 0.1$ for PEDOT:PSS molecules which changes from a stiff conformation at ϕ_{eff} = 0.01 (weaker screening) to a flexible coil conformation at ϕ_{eff} = 0.012 (larger screening, $0.1 < \kappa\xi < 1$). For PEDOT:PSS, l_e fluctuates between 2- 4 nm for concentrations upto ϕ_{eff} = 0.056 (For ϕ_{eff} > 0.056pH measurements became insensitive). It can also be observed that above the charge neutrality point (> 35 min), l_e starts to increase signifying a change in the conformation of the polymer. Since the release of counter-ions is the major reason behind the changes in the conformation, it may be concluded that the conformation of the PEC approaches linear extended state after 35 min drying. However, the continuously evaporating water environment reduces the counter-ion release and the conformational state is partially arrested after the charge neutralization point. The persistence length estimations carried out for dilute (ϕ_{eff} = 0.01) PEDOT:PSS dispersions in the presence of NaCl and $CuCl_2$ indicate (Table S1) more drastic changes in comparison to the H^+ fluctuations due to the evaporation of water. At the charge neutralization points, the l_e values of PEDOT:PSS with salt correspond to coiled conformations similar to the collapsed conformations observed in DNA in the presence of NaCl.[28] These suggest that the multi-region shear thinning behavior observed during the drying of PEDOT:PSS dispersion is due to the primary conformational changes induced by electrostatic interactions among the PEDOT:PSS PEC particles and the free PSS chains.

Table 4. Debye screening length (κ^{-1}), condition for screening ($\kappa\xi$) and electrostatic persistence length (l_e) for PEDOT:PSS during drying.

Drying Time	κ^{-1}	$\kappa\xi$	l_e
min	nm		nm
0	4.86	0.10	4.86
5	2.12	0.25	2.13
10	2.77	0.19	2.77
15	2.77	0.19	2.77
20	2.55	0.21	2.56
25	2.28	0.24	2.28
30	2.64	0.20	2.65
35	3.00	0.18	3.01
40	3.29	0.16	3.3
45	3.53	0.15	3.53

Is there a colloidal gel network formation and breakdown?

At higher concentrations (> 0.056), when the multi-region to single region shear thinning occurs, the dispersion behaves like a charged colloidal system. A colloidal system can be either dispersed or flocculated depending on the charge fluctuations in the solvent medium and the particle volume fraction.[29,30] The variation of storage modulus, *G'* and loss modulus, *G"* as a

function of increasing strain amplitude from 0.1 % to 100% are shown in Fig. 10. During the initial period of drying (ϕ_{eff} < 0.027), both *G′* and *G″* vary linearly with strain. As the ϕ_{eff} increased further, the linear viscoelastic limit shifted towards lower strain amplitudes.

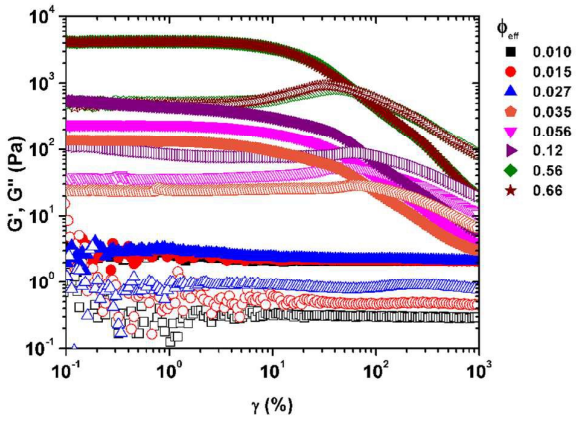

Fig. 10 Dynamic strain sweep for PEDOT:PSS dispersions during the drying process. The storage modulus *G′* (closed symbols) and the loss modulus *G″* (open symbols) at ω = 10 rad s^{-1}.

The strength of the bonds connecting the gel network can be predicted using the scaling concepts based on elastic properties of colloidal gels taking motivation from the scaling laws observed for polymer gels.[31] The scaling for the elastic modulus G_0', and the limit of linearity for the strain (γ_0) with respect to the particle volume fraction is dictated by the fractal nature of the colloidal flocs. A strong-linked and a weak-linked regime are found within and between colloidal flocs in gel networks.[31] Fig.11 (a) and (b) show the values of G_0' and γ_0.as function of effective volume fraction. Both G_0' and γ_0 show a power law behaviour and can be fitted to the forms $G_0' \sim \phi_{eff}{}^{1.3}$ and $\gamma_0 \sim \phi_{eff}{}^{0.5}$ indicating a weak-linked regime. This corroborates well with the steady shear and amplitude sweep studies where breakdown of networks was observed.

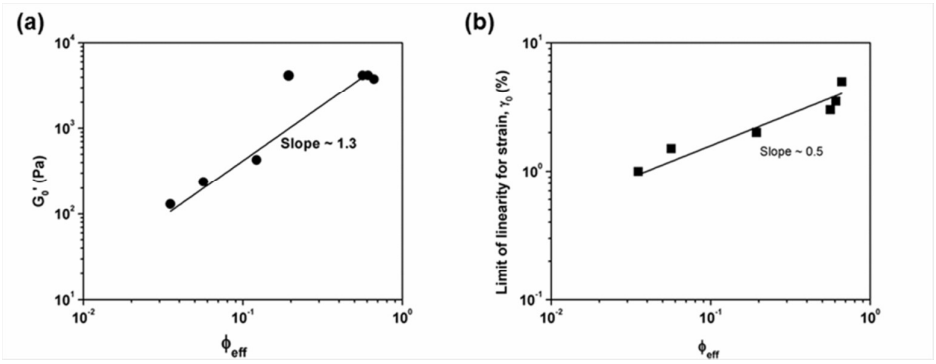

Fig. 11 (a). Variation of G_0' and (b) limit of linearity for strain, $\gamma_0$as a function of ϕ_{eff} for PEDOT:PSS dispersions

Proposed Mechanism

Fig. 12 shows the TEM micrographs of dried films of PEDOT:PSS from dispersions of very dilute concentrations and high concentrations. This along with the DLS data is used to arrive at the microstructural changes. At very low concentrations, 30-50 nm sized gel particles can be seen inside the aggregates which are ~ 250 nm size (these aggregates are from local drying during sample preparation, Fig. 12(a)) which can be confirmed from DLS data shown in Fig. 9 (inset). Earlier observations of thin films of PEDOT:PSS using TEM and STEM showed similar structures.[2,11,32,33] At higher concentrations, continuous network of aggregates form which is clearly visible in Fig. 12(b) which confirms the rheological findings at high concentrations.

From the steady shear and dynamic oscillatory shear experiments, TEM, particle size, Zeta potential and pH measurements, the following mechanism shown in Scheme 2 is proposed: (a) At ϕ_{eff} = 0.01 the electrostatic repulsion among the negatively charged PEC gel particles dominate; with linear, extended PSS anions in the medium, (b) for 0.01 <ϕ_{eff}< 0.027: evaporation of water shrinks the PEC; increase in the counter ions by the PSS chains and the capture by the PEC particle showing a shift from negative to positive zeta potential; linear extended PSS anions change to coiled conformation, (c) for 0.027 <ϕ_{eff}< 0.056: charge neutralization leading to the interplay of changes in conformation and aggregation behaviour, (d) ϕ_{eff} > 0.19: almost complete drying resulting in the formation of gel networks due to H-bonding involving adjacent PSS chains and PEC particles. The rheological behaviour also shifts from multi-region to single region shear thinning for concentrations > 0.056:

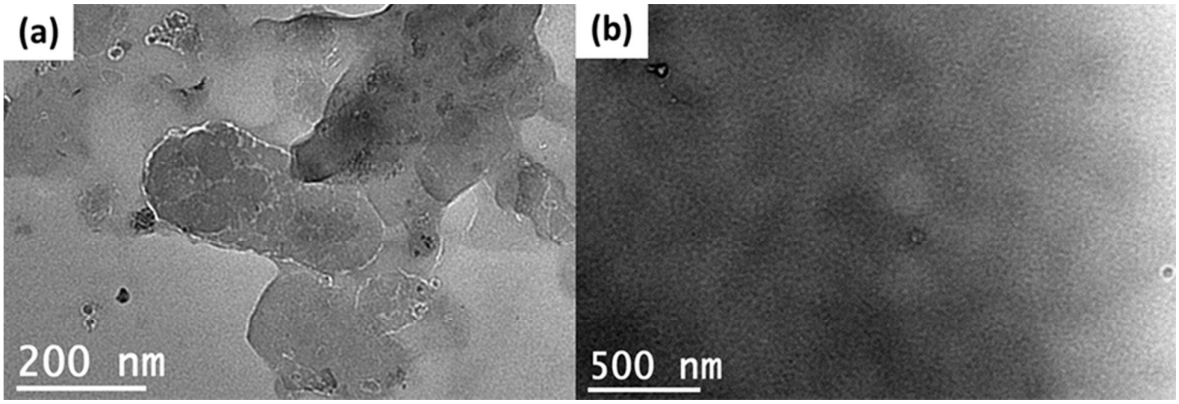

Fig. 12 TEM micrographs of dried films of PEDOT:PSS from dispersions of very dilute concentrations and high concentrations

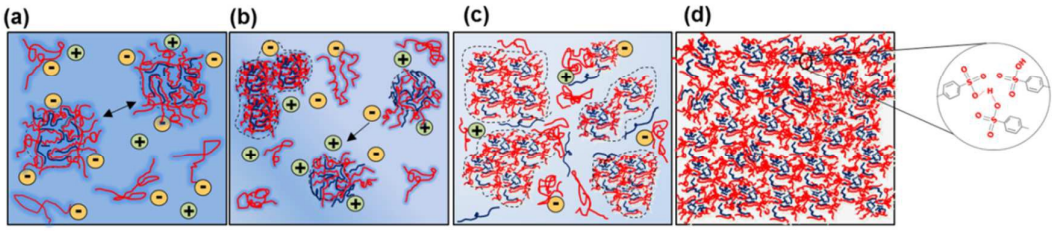

Scheme 2 Schematic representation of the conformational and microstructural changes of PEDOT:PSS during the drying process. Red and blue chains represent PSS molecules and PEDOT molecules respectively. Black dotted line denotes the hypothetical boundaries for PEC gel particle and aggregates. Green circles represent [H+] counter–ions and yellow circles represent [SO_3^-] anions. Fading blue background represents the evaporating water medium from the dispersion. (a) ϕ_{eff} = 0.01, (b) 0.01 <ϕ_{eff}< 0.027, (c) 0.027 <ϕ_{eff}< 0.056 and (d) ϕ_{eff} > 0.19

Conclusions

The microstructural contributions to rheology originating from conformational changes in the PEDOT:PSS molecules during the drying process are investigated. Steady shear experiments during the drying process revealed two distinct regimes in concentrations. Multiple shear thinning regimes along with Newtonian plateau observed at low effective volume fractions ϕ_{eff} are modeled using power law and the final phase showing a single shear thinning regime using Carreau model. Charge density fluctuations in PEDOT:PSS was found to play a key role in determining the conformational state of the PEC and the free PSS anions which determines the rheological behavior of the PEDOT:PSS at different ϕ_{eff}. The dispersions are found to shift from net negative to positive zeta potentials due to release and capture of counter-ions, during drying followed by charge neutralization. The charge neutralization during drying is found to be entropy-driven and is associated with dramatic increase in low shear viscosity and zero zeta potential indicating the formation of secondary aggregates. Electrostatic persistence length, l_e determined in the presence of salts and during the drying corroborated these observations. Dynamic shear of PEDOT:PSS dispersions at high ϕ_{eff} showed the transition from solid-like to gel-like network, characteristic of charged colloidal dispersions. Based on the scaling relations of colloidal gels, the gel network was found to be weak linked. TEM data and the particle size data from DLS strengthen the proposed mechanism of the microstructure evolution during the drying process. In summary, the conformational changes in PEDOT:PSS dispersion are governed by the charge density fluctuations during the initial period of drying however as drying progresses, the electrostatic interactions are taken over by the gel network formation and therefore behaves more like a weak-linked colloidal gel.

Acknowledgements

The authors acknowledge the financial support provided by the Department of Science and Technology, Government of India, and IITM-ARCI TEM facility for the TEM characterization

References

1 S.K.Andreas Elschner, Wilfried Lovenich, Udo Merker, and Knud Reuter In *PEDOT: Principles and Applications of an Intrinsically Conductive Polymer*, 1 ed.; CRC Press, Taylor and Francis Group: Boca Raton, FL, 2010; p 377.
2 A.M. Nardes, R.A.J. Janssen and M. Kemerink, *Adv. Funct. Mater.*2008**, 18**, 865-871.
3 S. Timpanaro, M. Kemerink, F. J. Touwslager, M. M. De Kok, and S. Schrader, *Chem. Phys. Lett.* 2004, **394**, 339-343.
4 Y. Xia and J. Ouyang, *Mater. Chem.* 2011**, 21**, 4927-4936.
5 J. Huang, P.F. Miller, J.C.de Mello, A. J. de Mello, and D.D.C. Bradley, *Synth. Met.*2003**, 139**, 569-572.

6 S. K. M. Jönsson, J. Birgerson, X. Crispin, G. Greczynski, W. Osikowicz, A. W. Denier van der Gon, W.R. Salaneck, and M. Fahlman, *Synth. Met.*2003**, 139**, 1-10.
7 P. Wilson, C. Lekakou, and J. F. Watts, *Org. Electron.* 2012**, 13**, 409-418.
8 D. Soltman and V. Subramanian, *Langmuir* 2008**, 24**, 2224-2231.
9 A. P. Erika Hrehorova, V.N. Bliznyuk and Paul D. Fleming In *Polymeric Materials for Printed Electronics and Their Interactions with Paper Substrates*, Proceedings of TAGA, 59th Annual Technical Conference, Pittsburgh, August, 2007; Pittsburgh, **2007**.
10 U. Lang, N. Naujoks andJ. Dual, *Synth. Met.*2009**, 159**, 473-479.
11 U. Lang, E. Müller, N.Naujoks, and J. Dual, *Adv. Funct. Mater.*2009**, 19**, 1215-1220.
12 H. Dautzenberg, *Macromolecules* 1997**, 30**, 7810-7815.
13 H. Yan, S. Arima, Y. Mori, T.Kagata, H. Sato, and H. Okuzaki, *Thin Solid Films* 2009**, 517**, 3299-3303.
14 N. J. W. Jan Mewis, In *Colloidal Suspension Rheology*, Cambridge University Press: New York, 2012; p 416.
15 G. Harrison, G. V. Franks, V. Tirtaatmadja, and D. V. Boger, D. V. *Korea-Aust. Rheol. J.*1999**, 11**, 197-218.
16 S. D. Hoath, S. Jung, W. K. Hsiao, and I. M. Hutchings, *Org. Electron.* 2012**, 13**, 3259-3262.
17 M. R. Erika Hrehorova, Alexandra Pekarovicova; P. D. Fleming, and V. N. Bliznyuk. *TAGA Journal of Graphic Technology* 2007**, 4**, 13.
18 L. Yang, B. K. Kazmierski, S. D. Hoath, S. Jung, W. K. Hsiao, Y. Wang, A. Berson, O. Harlen, N. Kapur, and C. D. Bain, *Physics of Fluids* 2014**, 26**, 113103
19 D. Bagchi and R. Menon, *Chem. Phys. Lett.* 2006,**425**, 114-117.
20 R.Borrega, R.Cloitre, I.Betremieux, B.Ernst and L. Leibler, *Europhys. Lett.* 1999, **47**, 729-735
21 L. Jin, Y. Tan, Y.Shangguan, Y. Lin, B. Xu, Q. Wu, and Q. Zheng, *J. Phys. Chem. B*2013**,117**, 15111-15121.
22 V. Burckbuchler, A. L.Kjøniksen, C. Galant, R. Lund, C. Amiel, K. D. Knudsen, and B. Nyström, *Biomacromolecules* 2006**,7**, 1871-1878.
23 L. M. Walker, N. J. Wagner, R. G. Larson, P. A. Mirau, P.J. Moldenaers, *Rheo.*1995**,39**, 925-952.
24 Y. Xia, and J. Ouyang, *Macromolecules* 2009**, 42**, 4141-4147.
25 A. Thünemann, M. Müller, H.Dautzenberg, J. F. Joanny, and H.Löwen, Polyelectrolyte Complexes. In *Polyelectrolytes with Defined Molecular Architecture II*, Schmidt, M., Ed. Springer Berlin Heidelberg: 2004; Vol. **166**, pp 113-171.
26 O. P .Dimitriev, Y. P. Piryatinski, and A. A. Pud, *J. Phys. Chem. B* 2011**,115**, 1357-1362.
27 B. Y. Ha, and D. Thirumalai, *Macromolecules* 1995**, 28**, 577-581.
28 R.W. Wilson, D. C. Rau, and V. A. Bloomfield, *Biophys. J.* 1980**, 30**, 317-325.
29 D. A. R. Jones, B. Leary, and D. V. Boger, *J. Colloid Interface Sci.* 1991**,147**, 479-495.
30 A. Hess, M.Pretzl, L.Heymann, A.Fery, and N. Aksel, *Physical Review E* 2011**,84,** 031407
31 W. H. Shih, W. Y. Shih, S. I. Kim, J. Liu, and I. A. Aksay, *Phys. Rev. A* 1990**, 42**, 4772-4779.
32 H.Yan, S.Arima, Y.Mori, T.Kagata, H.Sato and H.Okuzaki, *Thin Film Solids,* 2009, **517**, 3299-3303
33 .Zhou, D.H. Anjum, L. Chen,X. XuI. A Ventura, L. Jiangand G. Lubineau, *J.Mat.Chem. C.,* 2014, **2,** 9903.

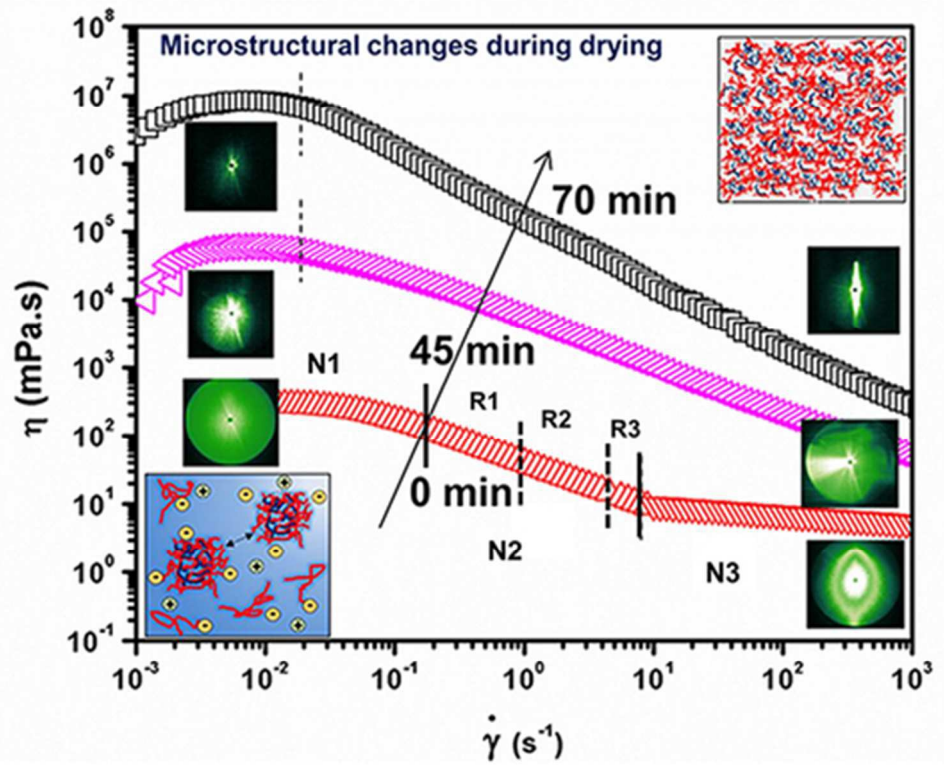

39x32mm (300 x 300 DPI)